ACS OMEGA

http://pubs.acs.org/journal/acsodf

Article

Prediction of Power Conversion Efficiencies of Diphenylthienylamine-Based Dyes Adsorbed on the Titanium Dioxide Nanotube

Ohoud S. Al-Qurashi and Nuha Wazzan*

Cite This: *ACS Omega* 2021, 6, 8967−8975

Read Online

ACCESS | Metrics & More | Article Recommendations | Supporting Information

ABSTRACT: The power conversion efficiency (η) is the most important key to determine the efficiency of dye-sensitized solar cell (DSSC) devices. However, the calculation of η theoretically is a challenging issue since it depends on a large number of experimental and theoretical parameters with extensive related data. In this work, η was successfully predicted using the improved normal model with density functional theory (DFT) and time-dependent density functional theory (TD-DFT) for eight diphenylthienylamine-based (DP-based) dyes with various π-bridge adsorbed on titanium dioxide. The titanium dioxide is represented by a nanotube surface (TiO_2NT); this surface is rarely investigated in the literature. The π-linker consists of five (DP1)- or six (DP2)-membered rings and contains none to three nitrogen atoms (D0−D3). The reliability of the estimated values was confirmed by the excellent agreement with those available for the two experimentally tested ones (DP2-D0 and DP2-D2). The deviations between the experimental and estimated values were in the ranges of 0.03 to 0.06 mA cm^{-2}, 0.05 to 0.3 mV, and 0.37 to 0.18% for short-circuits current density (J_{sc}), open-circuit voltage (V_{oc}), power conversion efficiency (%η), respectively. More importantly, the results revealed that using pyridine (DP2-D1), pyrimidine (DP2-D2), and 1,2,4-triazine (DP2-D3) improves the power conversion efficiencies in the range of 6.03 to 6.90%. However, the cyclopenta-1,3-diene (DP1-D0) shows superior performance with a predicted η value that reaches 9.55%.

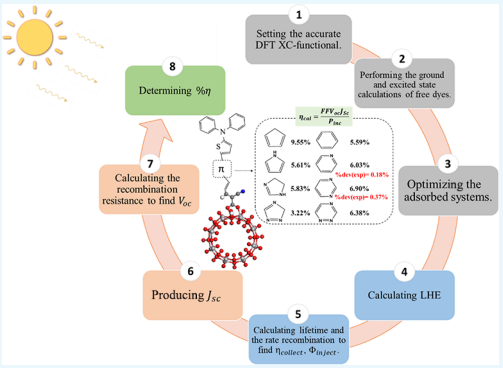

1. INTRODUCTION

In the last three decades, Grätzel cells, often referred to as dye-sensitized solar cells (DSSCs),[1] have been widely studied experimentally and theoretically. The working mechanism of the DSSC includes many processes such as the photoinduced, injection, and regeneration processes. Among the different compositions of DSSCs, the development of an efficient dye and semiconductor has attracted the attention of researchers in order to improve the overall power conversion efficiency of the DSSC.[2−7] The TiO_2-based DSSC was found to be an appropriate photoelectrode compared to other metal oxide semiconductors due to its wide band gap. Particularly, the TiO_2 nanotube (TiO_2NT) can reduce the recombination possibilities and leads to higher efficiency than bulk TiO_2. It has unique optical properties such strong adsorption capacity, better electron transference paths, high electron mobility, and increased charge transport capacity. This nanostructured TiO_2 can attach and adsorb different potential materials. However, up to now, the investigation of its profound structures and applications has not been fully explored.[8] Maybe the work of Hoyer[9] was the first effort to produce titania nanotubes. After that, several attempts were used to prepare TiO_2 nanotubes, and the synthesis methods included the electrochemical deposition method, sol−gel techniques, hydro/solvothermal methods, and so on.[8] The first attempt to synthesize TiO_2NT-based DSSCs was in 2005 by Macák and his co-workers.[10] After that, various theoretical studies have attempted to investigate the structural and electronic properties of TiO_2NTs in different fields.[11−15]

The highest power conversion efficiency (η) of a DSSC reached 16.5%.[16] This parameter strongly depends on the short-circuit current (J_{sc}), open-circuit photovoltage (V_{oc}), and fill factor (FF). In DSSCs, the open-circuit voltage is known as the difference between the redox potential of the electrolyte and the Fermi level of the semiconductor (see Figure S1). Short-circuit current density is the ability to inject an electron into the conduction band of the semiconductor and the ability to transfer an electron to the collecting electrode. However, the fill factor reduces the actual power taken into account $J_{sc} \times V_{oc}$[17] and is defined by the ratio of the maximum power (P_{max}) of the solar cell per unit area divided by J_{sc} and V_{oc}.[18]

Received: December 30, 2020
Accepted: March 11, 2021
Published: March 27, 2021

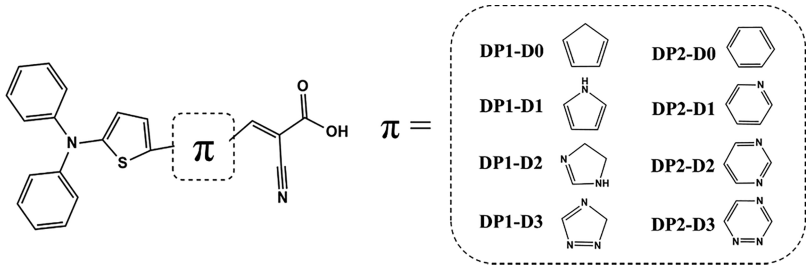

Figure 1. Chemical structures of the DP-based dyes.

Numerous works researched the possibility of enhancing the short-circuit current by studying serval factors such as light-harvesting and lifetimes and the injection and regeneration driving forces (see Section 3.2 and Scheme 2). The light-harvesting efficiency is affected by the molar absorption coefficient and dye loading amount. Improving the short-circuit current causes the development of the open-circuit photovoltage and power conversion efficiency. However, through the photoexcitation process, the excited electron could recombine with the HOMO level of the oxidized sensitizer or with the electrolyte. This recombination process competes with the desired dye regeneration process between the electrolyte and the HOMO level of the dye, leading to reduced short-circuit current.[19]

Venkatraman and co-workers[20] found that the planarity and degree of aromaticity for furan-, pyrrole-, thiophene-, pyridine-, and benzene-based π-linkers are impacted by the driving forces that will influence the short-circuit current. Lu and his collaborators[21] investigated the effect of using pyridinium ylide as an anchor unit on the photochemical and photophysical characteristics. Their results revealed that using pyridinium ylide enhanced the light-harvesting and thus led to improved electron injection through the photoanode. Therefore, it exhibited increasing values in J_{sc} and V_{oc}. Based on the research of Wang et al.,[22] it was observed that the inserted graphene layer between the photoanode and dyes has influenced the electron injection process to the conduction band, which improves the J_{sc} value due to the acceleration of electron injection lifetimes in their systems. Murakami and co-workers[23] found that using triphenylamine as a donor unit produces higher J_{sc} and V_{oc} due to longer recombination electron lifetime as a result of the blocking effect of the donor.

The use of experimental methods to analyze dyes for DSSCs proved to be time-and cost-inefficient. In such experiments, the architecture of existing compounds was identified and systematically changed, and the suitability of the new compounds can be tested only by applying these compounds in real applications. This procedure is usually a hit-or-miss procedure that often leads to unpleasing results. Therefore, there is an essential need to understand the properties of the dyes at a molecular level and modify the architecture of existing dyes with promising units before proceeding with experimental testing. Several useful parameters of the designed dyes have been successfully evaluated theoretically, which were used to assist the validity/potential of such dyes if they are used in real applications. Such parameters included the critical geometrical parameters, electronic properties, etc. However, the key parameters related to PCE including the total power conversion efficiency (η), short-circuits current density (J_{sc}), open-circuit voltage (V_{oc}), light-harvesting efficiency (LHE) are extremely important to predict the designed dyes' performances in real applications.

Few theoretical efforts have attempted to predict the values J_{sc}, V_{oc}, and η. Recently, Zhao and co-workers[24] studied four triazatruxene-based dyes by modified π-linker and anchoring units using density functional theory (DFT) and time-dependent density functional theory (TD-DFT). Comprehensive calculations were carried out to predict the PCE parameters. The results revealed that the highest η (16.7%) was demonstrated by furan and cyanoacetic acid as spacer and anchoring groups. At the same time, they introduced graphene quantum dots to those dyes. It was found that insertion of the graphene led to an increase in the η value at a maximum of 0.7% compared with free graphene dyes. Based on the IQ1 sensitizer, Xu et al.[25] designed a series of metal-free sensitizers theoretically by adjusting the acceptor fragment. This strategy enhanced the light-harvesting and caused an increase in the conduction band edge of the semiconductor. Consequently, the J_{sc} and V_{oc} becomes higher, which improved the performance of η. In a study of the effect of anionic tetrazolyl-based ligands on Ru(II) complex dyes, the computed J_{sc} values using the PBE0 functional and LanL2DZ basis set were well-matched with the corresponding experimental values with differences of 0.46 and 2.82 mA cm^{-2} for BMTP and BTP, respectively. The accuracy of the selected DFT-functional (PBE0/LanL2DZ) used in that study was proven by the good matching between the calculated and the experimental wavelengths, resulting in an excellent estimation of the J_{sc} value.[26] Similarly, the calculated J_{sc} values of five triarylamine-based dyes, abbreviated as A1, A1-F, C218, D2, and Y123, were in an excellent agreement with the experimental data when the CAM-B3LYP/DGDZVP was applied.[27] Ma et al.[28] have successfully predicted η with deviations of 1−2% for three ullazine dyes (JD32), and the three dyes contain triphenylamine and cyanoacrylic acid as the donor and acceptor units (L-dyes) using the improved normal model to find V_{oc}. As well, they proved that using the normal model to estimate V_{oc} led to nearly 2 times larger than that of the experiment results, and details of these two equations are provided in Section 3.3. This also was found in the study of the C281 dye, in which the predicted η overestimated the experimental value with a difference of 7.3% when using the normal model.[29]

In this effort, to find promising candidates for efficient DSSCs, a series of dyes have been designed based on DP-based dyes (see Figure 1). DP-based dyes are constructed of diphenylthienylamine (DP) as the donor unit and cyanoacrylic acid as the anchoring unit. The study included their adsorption on the $(TiO_2)_{32}$ surface. The titanium dioxide is represented by a nanotube surface (TiO_2NT). This surface is rarely investigated in the literature.[13] The difference among them is

https://doi.org/10.1021/acsomega.0c06340
ACS Omega 2021, 6, 8967−8975

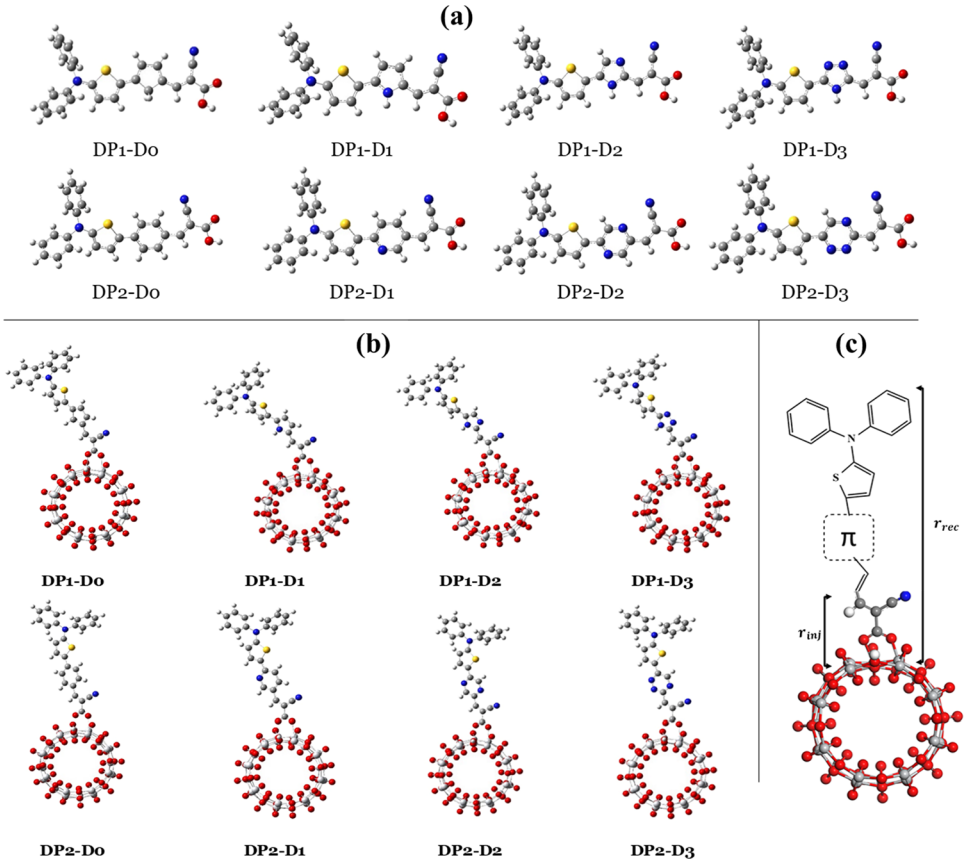

Figure 2. Optimized geometries of (a) free dyes, (b) the adsorbed dyes on the TiO_2NT and (c) illustration of the electron recombination (r_{rec})/injection (r_{inj}) distances.

in the π-bridge, which are five (DP1)- and six-membered rings (DP2) without/with nitrogen atoms such as cyclopenta-1,3-diene (DP1-D0), pyrrole (DP1-D1), imidazole (DP1-D2), 3*H*-1,2,4-triazole (DP1-D3), benzene (DP2-D0), pyridine (DP2-D1), pyrimidine (DP2-D2), and 1,2,4-triazine (DP2-D3). Also, the results will be compared with the results of the two experimentally tested dyes DP2-D0 and DP2-D2.[30]

The purpose of this study is to give details on how to predict the power conversion efficiencies of eight DP-based dyes and analyze the factors affecting these values using density functional theory and time-dependent density functional theory. The reliability of the obtained results will be supported by comparing the estimated data with the corresponding available experimental data for the two dyes DP2-D0 and DP2-D2.[30] The chemical structures of the studied dyes and the optimized geometries of free and adsorbed dyes on TiO_2NT are depicted in Figures 1 and 2, respectively. The computational workflow that was used to achieve reliable prediction of power conversion efficiencies is presented in Scheme 1.

Scheme 1. Computational Workflow for Calculated Prediction of Power Conversion Efficiencies

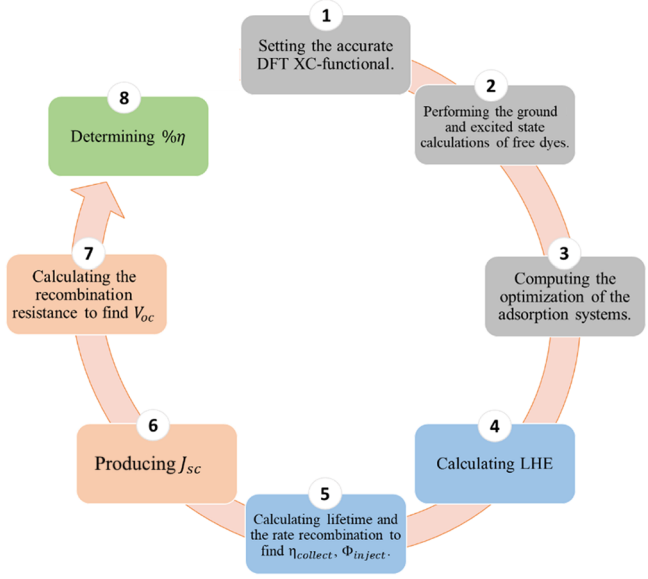

2. COMPUTATIONAL DETAILS

The geometrical structures of the isolated dyes were calculated using the Becke three-parameter exchange functional and the Lee−Yang−Parr correlation functional (B3LYP).[31,32] The Pople split-valence double-zeta basis set with d and p polarization orbitals and enlarged with one type of diffuse function, i.e., the 6-31G+(d,p) basis set, was chosen. The solvation effects were simulated using the polarized continuum model (PCM)[33−35] in acetonitrile (CH_3CN ε = 37.5). The TD-DFT calculations were employed to simulate the absorption and emission spectra by the hybrid exchange-correlation functional (CAM-B3LYP)[36] that displays better agreement with the two experimental maximum absorption wavelengths of the DP2-D0 and DP2-D2 dyes.[30] In comparison with five DFT XC-functionals, the CAM-B3LYP/6-31G+(d,p) displayed the smallest % deviations

https://doi.org/10.1021/acsomega.0c06340
ACS Omega 2021, 6, 8967−8975

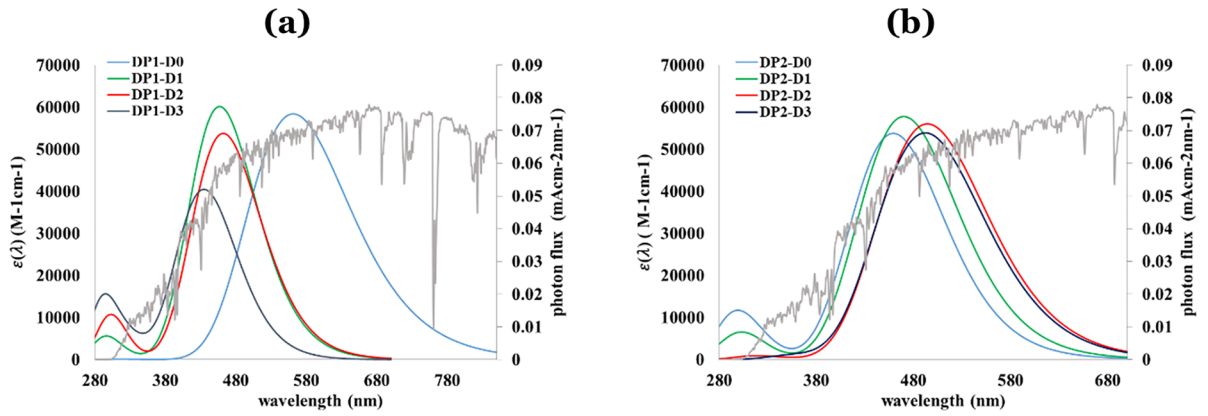

Figure 3. Simulated UV−vis absorption of (a) DP1-dyes and (b) DP2-dyes by the Air Mass 1.5 Global (AM 1.5G) solar spectrum (gray line) as computed at the PCM/TDCAM-B3LYP/6-31G+(d,p) levels of theory in acetonitrile solvent.

equaling 5 and 3% for the two dyes, respectively (for more details, see the Supporting Information).

The geometries of adsorbed dyes on the titanium dioxide $(TiO_2)_{32}$ nanotube (TiO_2NT) were fully optimized using the 6-31G(d) basis set for all atoms except the Ti atom in the Los Alamos National Laboratory with the double zeta (DZ) (LANL2DZ) and pseudopotential basis set for the Ti atom.[37] All the DFT calculations were applied using Gaussian 09 suite programs,[38] and visual inspections were performed using the GaussView program (version 5.0.8).[39]

3. RESULTS AND DISCUSSION

3.1. Light-Harvesting Efficiency. The light-harvesting efficiency (LHE) is an essential property in DSSCs and plays a key role in improving J_{sc} and thus increasing η. To estimate the LHEs of the eight dyes, UV−vis absorption spectra were simulated as shown in Figure 3 since the LHE can be calculated according to the following equation[40]

$$\mathrm{LHE}\ (\lambda) = 1 - 10^{-\varepsilon(\lambda)\Gamma} \tag{1}$$

where $\varepsilon(\lambda)$ is the molar absorption coefficient at the specific wavelength calculated from TD-DFT. Γ is the dye loading amount ($\Gamma = c \cdot b$), corresponding to the result of multiplication of the dye concentration (c) with TiO_2 film thickness (b), and it was taken from the experimental data (2.50×10^{-7} mol cm^{-2}).[30]

As can be noted from Table 1, the LHE values for the eight dyes are greater than 90%, except DP1-D3, which has the smallest LHE value of 82% due to its lower ε value. As known, the larger molar absorption coefficient will result in a large value of LHE. This observation is noted in DP1-D0 that shows the largest molar absorption coefficient of 6.34×10^6 M^{-1} cm^{-1} and thus exhibits the largest LHE among the eight dyes. Overall, all dyes can efficiently harvest sunlight to produce electricity.[41]

The injection lifetime of the excited state (τ_{inj}) is another key factor that influences the efficiency of the DSSC through the enhancement of electron injection and exciton dissociation processes. It is known as the average time that electrons spend in the LUMO before emitting to the CB of the semiconductor (eq 2).[42] On the other hand, the recombination lifetime (τ_{rec}) denotes the average time to transfer electrons from the CB to the redox potential of the electrolyte. As reported in the literature, a shorter value of the injection lifetime and a larger value of the recombination lifetime result in improving the performance of DSSCs.[23,43,44]

Table 1. Maximum Absorption λ_{abs} and Maximum Emission Wavelengths λ_{em} (/nm), the Molar Absorption Coefficient $\varepsilon(\lambda)$ ($\times 10^6$/M^{-1} cm^{-1}), the Light-Harvesting Efficiency (LHE), Oscillator Strengths (f_{em}), and Fluorescence Energy E_{flu} (/eV), as Calculated at the PCM/TD-CAM-B3LYP/6-31G+(d,p) in Acetonitrile Solvent

dye	λ_{abs}	$\varepsilon(\lambda)$	λ_{em}	E_{flu}	f_{em}	LHE
DP1-D0	561.24	6.34	694.49	1.785	1.580	0.974
DP1-D1	456.69	4.86	569.67	2.177	1.722	0.939
DP1-D2	461.82	4.49	588.74	2.106	1.623	0.925
DP1-D3	434.54	3.05	551.05	2.250	1.323	0.828
DP2-D0	459.23	4.33	582.50	2.129	1.781	0.918
DP2-D1	470.00	4.77	573.85	2.161	1.806	0.936
DP2-D2	494.26	5.28	609.70	2.034	1.716	0.952
DP2-D3	492.19	5.61	613.81	2.020	1.680	0.960

$$\tau_{inj} = \frac{c^3}{2(E_{flu})^2 f_{em}} \tag{2}$$

where c is the light speed, E_{flu} is the fluorescence energy, and f_{em} is the oscillator strength all in a.u. units. The eight dyes' lifetime values are listed in Table 2, and their emission spectra are presented in Figure S2. The faster lifetimes are noted for DP1-D0 with a value of 0.429 ps. Generally, it is found that the values of τ_{inj} increase with the incorporation of the nitrogen atoms in the π-linker up to three nitrogen atoms, which will improve the charge transfer capacity of dyes. Therefore, this enhancement in the values of τ_{inj} will develop the J_{sc} as will be proven and discussed in Section 3.2.

3.2. Short-Circuit Current Density. To estimate the photoelectric conversion efficiency, the short-circuit current density (J_{sc}) should be first estimated and can be determined according to the following equation[45]

$$J_{sc} = e \int \mathrm{LHE}\ (\lambda)\phi_{inj}\eta_{coll}\varphi_{ph.AM1.5G}(\lambda)\mathrm{d}(\lambda) \tag{3}$$

where LHE(λ) is available from Table 1. $\varphi_{ph.\ AM1.5G}$ is a standard reference for the solar-radiation intensity in unit mA cm^{-2} nm^{-1}. Meanwhile, Φ_{inj} is the electron injection efficiency,[46] and η_{coll} is the charge collection efficiency.[47] They are defined as

https://doi.org/10.1021/acsomega.0c06340
ACS Omega 2021, 6, 8967−8975

Table 2. Free Energy of Dye Regeneration (ΔG_{reg}/eV), the Total Reorganization Energy (λ_{tot}/eV), the Activation Energy of the Recombination Process, Electron Recombination Distance (r_{rec}/Å), the Electron Injection Efficiency Φ_{inj}, the Rate Recombination (k_{rec}/s^{-1}), the Charge Collection Efficiency η_{coll}, the Electron Lifetimes τ_{inj} (/ps), the Electron Recombination Lifetime τ_{rec} (ns), the Photon Flux $\varphi_{ph.\ AM1.5G}$ (mA cm^{-2} nm^{-1}), and Short-Circuit Current Density (J_{sc}/mA cm^{-2})

dye	ΔG_{reg}	λ_{tot}	ΔG^{*}_{reg}	r_{rec}	k_{rec} (10^7)	Φ_{inj}	τ_{inj}	τ_{rec}	η_{coll}	$\varphi_{ph.\ AM1.5G}$ (10^{-2})	J_{sc}
DP1-D0	−0.43	0.604	1.25×10^{-2}	16.54	6.22	0.959	0.429	0.161	1.00	7.08	18.54
DP1-D1	−0.47	0.630	1.02×10^{-2}	16.19	8.91	0.935	0.695	0.112	1.00	5.80	11.61
DP1-D2	−0.54	0.636	3.62×10^{-3}	16.55	6.90	0.942	0.614	0.145	1.00	5.90	11.87
DP1-D3	−0.66	0.614	8.62×10^{-4}	16.82	4.70	0.946	0.571	0.213	1.00	3.98	6.77
DP2-D0	−0.55	0.567	1.27×10^{-4}	16.25	4.07	0.936	0.688	0.245	1.00	5.71	11.25
DP2-D1	−0.63	0.548	3.07×10^{-3}	16.99	2.52	0.933	0.719	0.397	1.00	5.73	11.75
DP2-D2	−0.71	0.588	6.33×10^{-3}	16.63	4.57	0.943	0.605	0.219	1.00	6.20	13.75
DP2-D3	−0.80	0.625	1.23×10^{-2}	16.65	7.05	0.945	0.584	0.142	1.00	5.92	13.21

$$\Phi_{inj} = 1/\left(1 + \frac{\tau_{inj}}{\tau_{relx}}\right) \quad (4)$$

$$\eta_{coll} = 1/\left(1 + \frac{\tau_{trans}}{\tau_{rec}}\right) \quad (5)$$

The electron injection lifetime is the same value as the inverse electron injection rate k_{inj}. It is noted that τ_{inj} gives more accurate results than the inverse electron injection rate k_{inj}. τ_{relx} is the relaxation time for the dye excited state that was taken from the experimental value of ∼10 ps,[48] and τ_{trans} is the electron transport time for electrons from TiO_2 to I^-/I_3^-. As well, the electron recombination lifetime matches the inverse of the rate recombination k_{rec}. Both the electron injection and recombination rates (k_{ET}) can be obtained from the Marcus theory[49,50] as

$$k_{ET} = \sqrt{\frac{\pi}{\hbar \lambda_{tot} k_B T}} \exp^{(-\beta r)} \exp^{[-(-\Delta G^{*} + \lambda_{tot})^2 / 4\lambda_{tot} k_B T]} \quad (6)$$

The left side of the equation represents the reduced Planck constant $\hbar$ (6.5821 ×10^{-16} eV s), the total reorganization energy (λ_{tot}), the Boltzmann constant k_B (8.6173 ×10^{-5} eV K^{-1}), and the absolute temperature T (300 K). The right side shows an attenuation factor β that is equal to 0.5, r is the electron-transfer distance (the distance from the anchoring group and from the donor unit to the TiO_2 surface in the injection and recombination processes, respectively, see Figure 2c), and finally, ΔG^{*} refers to the activation energy for the reaction that depends on driving forces ΔG^{o}, which can be calculated according to the following equation[51]

$$\Delta G^{*} = \frac{-(-\Delta G^{o} + \lambda_{tot})^2}{4\lambda_{tot}} \quad (7)$$

As can be noted from Table 2, the photon flux shows a significant effect on the J_{sc} compared to the other parameters since the increase in the photon flux leads to a higher value of J_{sc}. For instance, the photon fluxes of the DP1-D0 and DP1-D3 dyes are 7.08 ×10^{-2} and 3.98 ×10^{-2} mA cm^{-2} nm^{-1}, and their J_{sc}s are 18.54 and 6.77 mA cm^{-2}, respectively. This means that the J_{sc} strongly depended on the LHE and the wavelengths. Furthermore, the J_{sc} increases with the addition and increases the number of nitrogen atoms.

The incident photon to charge carrier efficiency (%IPCE) is calculated using the following equation[52] and presented graphically in Figure 4.

$$\%IPCE = \frac{1240 \times J_{sc}}{\lambda_{abs} \times \phi_{ph}^{source}} \times 100 \quad (8)$$

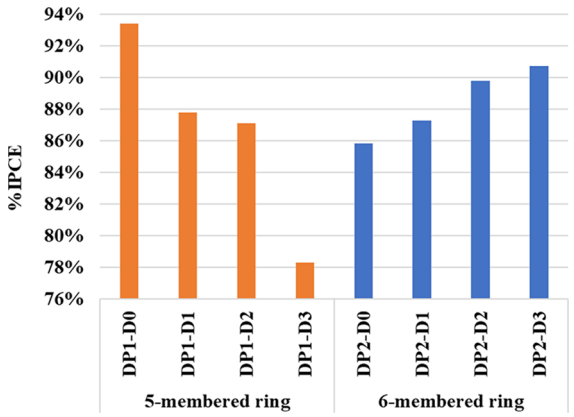

Figure 4. Percentage of the incident photon to charge carrier efficiency %IPCE of the five- and six-membered-ring dyes.

where ϕ_{ph}^{source} is equal to 100 mW cm^{-2}. As well, the following equation can be used to calculate %IPCE[53]

$$\%IPCE = (LHE\ (\lambda) \phi_{inj} \eta_{coll}) \times 100 \quad (9)$$

Equation 8 exhibits that %IPCE is directly proportional to J_{sc}. As mentioned in Section 3.2, DP1-D0 shows the largest J_{sc}, and thus, it is expected that it will have the highest %IPCE. Obviously, from Figure 4, it can be seen that the addition of nitrogen atoms in the DP1 dyes leads to a decrease in %IPCE while in the DP2 dyes, and the opposite trend is noted. The % IPCEs of the eight studied dyes fall in range of 78−93%, and it increases in the order of DP1-D0 > DP2-D3 > DP2-D2 > DP1-D1 > DP2-D1 = DP1-D2 > DP2-D1 > DP1-D3. The %IPCEs of DP2-D0 and DP2-D2 are in excellent agreement with the experimental data,[30] which ensures the applied theoretical calculations' accuracy and reliability.

3.3. Open-Circuit Photovoltage. Once the J_{sc} is estimated, the open-circuit photovoltage (V_{oc}) can also be estimated applying the normal model[54] (eq 10) or the improved normal model (eq 11).[17]

$$V_{oc} = \frac{E_c + \Delta CB}{q} + \frac{k_B T}{q} \ln\left(\frac{n_c}{N_C}\right) - \frac{E_{redox}}{q} \quad (10)$$

where E_c is the conduction band edge of the semiconductor, ΔCB is the shift of E_c when the dyes are adsorbed on the

https://doi.org/10.1021/acsomega.0c06340
ACS Omega 2021, 6, 8967−8975

semiconductor surface, q is the electron charge, n_c is the number of electrons in the conduction band, N_C is the accessible density, and E_{redox} is the reduction−oxidation potential.

As mentioned early in Section 1, eq 10 was proven to be less accurate than eq 11. This is because the normal model neglects the energy loss and thus produces an unreliable value of η. Energy loss is known as the difference between V_{oc} and the lowest energy band gap of the donor/acceptor fragments.[55] The electron may recombine with the electrolyte or holes through the electron injection process, leading to a reduction in Fermi energy of the semiconductor and hence a reduction in V_{oc}. Accordingly, the energy loss and recombination effect must be measured to predict V_{oc}, where they are considered in the improved normal model.[28] Thus, in this work, the improved normal model was used, and its results are listed in Table 3.

$$V_{oc} = \frac{k_B T}{\beta'} \ln \frac{\beta' R_0 J_{sc}}{k_B T} \tag{11}$$

Table 3. Shift of CB (E_{CBM}/eV), the Recombination Resistance (R_0/Ω cm^2), and Open-Circuit Photovoltage (V_{oc}/mV)

dye	E_{CBM}	R_0	V_{oc}
DP1-D0	−3.075	1.13×10^3	0.74
DP1-D1	−3.081	8.15×10^2	0.69
DP1-D2	−3.090	9.68×10^2	0.70
DP1-D3	−3.100	1.17×10^3	0.68
DP2-D0	−3.096	1.18×10^3	0.71
DP2-D1	−3.099	1.72×10^3	0.73
DP2-D2	−3.099	1.10×10^3	0.72
DP2-D3	−3.111	7.13×10^3	0.69

where β' is the charge transfer coefficient for the recombination process and is equal to 0.45 and R_0 is the recombination resistance that can be predicted as[56]

$$R_0 = \frac{\sqrt{\pi \lambda k_B T}}{q^2 d \gamma k_{rec} c_{ox} N_s} \exp\left(\gamma \frac{E_{CBM} - E_{redox}}{k_B T} + \frac{\lambda_{tot}}{4 k_B T}\right) \tag{12}$$

where d is the film thickness that is taken from the experimental value of 10 μm,[30] γ is the electron trap distribution below the CB and takes a value of ∼0.3,[28] c_{ox} is the concentration of acceptor species (I_3^-∼50 mmol L^{-1}), N_s is the total number of surface states contributing to recombination and set to be ∼10^5, E_{CBM} is the shift of the CB after the dye adsorbed on TiO_2, and E_{redox} is the reduction−oxidation potential and takes a value of −5.08 eV (see Figure S3).

According to the photocurrent-photovoltage properties of solar cells, we can correlate V_{oc} with J_{sc}. The influence of the recombination process on V_{oc} should be considered. V_{oc} could be defined as the maximum difference between the Fermi level of electrons in the TiO2NT and the electrochemical potential of the holes in hole transfer materials represented here by the redox potential of the I^-/I_3^-. Due to the fact that the holes and electrons are nearby to each other in the nanostructured configuration of the DSSC, the electrons can recombine with the holes in the dyes or in the I^- ion. This recombination will result in a lowering Fermi level of electrons in the TiO2NT; therefore, the value of V_{oc} decreases due to the electron−hole recombination.[28]

We found that the recombination resistance is strongly dependent on E_{CBM} and mainly influence V_{oc} values,[28] i.e., a less negative value of E_{CBM} will lead to improving V_{oc}. Generally, in the six-membered-ring dyes, the V_{oc} values are higher than the values for their corresponding five-membered rings. Nevertheless, DP1-D0 shows the highest value due to its lowering E_{CBM} value.

Scheme 2. Factors Affecting the Power Conversion Efficiency (η)

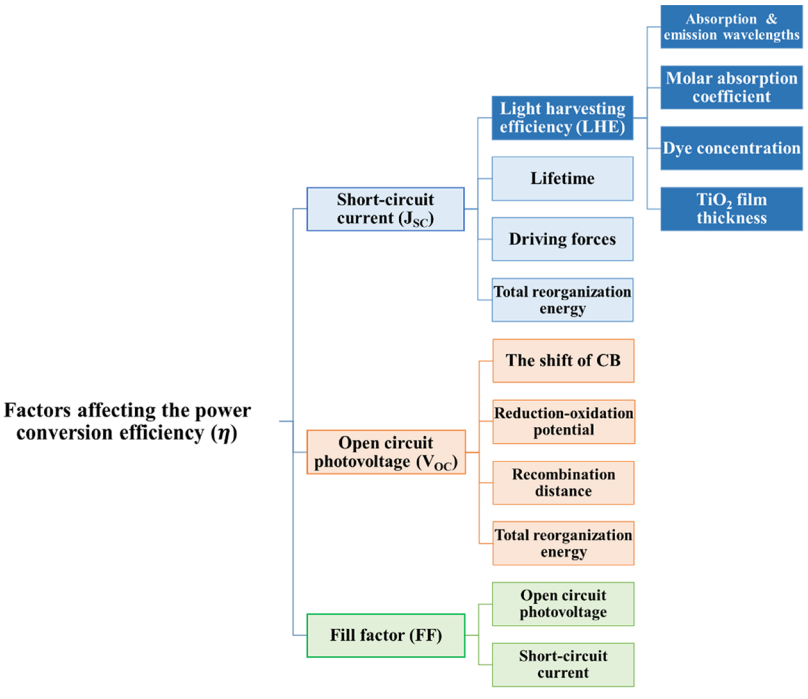

https://doi.org/10.1021/acsomega.0c06340
ACS Omega 2021, 6, 8967−8975

3.4. Power Conversion Efficiency. The power conversion efficiency (η) is the final key to determining the overall performance of DSSC devices, and its value is determined by various photovoltaic parameters, which are illustrated in Scheme 2. It can be predicted using the following equation

$$\eta = \frac{\mathrm{FF} V_{oc} J_{sc}}{P_{inc}} \quad (13)$$

where FF is the fill factor, and it was taken from the experiment (0.70),[30] and P_{inc} is incident sunlight and it is equal to 100 mW cm^{-2}.

Table 4 presents a comparison between the theoretical and the available experimental data[30] for J_{sc}, V_{oc}, and %η for the

Table 4. Theoretical Open-Circuit Photovoltage (V_{oc}/ mV), Short-Circuit Density (J_{sc}/mA cm^{-2}), and the Power Conversion Efficiency (%η)

	predicted value			experimental value[a]		
dye	J_{sc}	V_{oc}	%η	J_{sc}	V_{oc}	%η
DP1-D0	18.54	0.74	9.55			
DP1-D1	11.61	0.69	5.61			
DP1-D2	11.87	0.70	5.83			
DP1-D3	6.77	0.68	3.22			
DP2-D0	11.25	0.71	5.59	11.19	0.66	5.22
DP2-D1	11.75	0.73	6.03			
DP2-D2	13.75	0.72	6.90	13.72	0.69	6.72
DP2-D3	13.21	0.69	6.38			

[a]Experimental values from ref 30.

DP2-D0 and DP2-D2 dyes. Remarkably, the three estimated parameters displayed very small deviations from their corresponding experimental values. The deviations fall in the range of 0.03 to 0.06 mA cm^{-2}, from 0.05 to 0.3 mV, and from 0.37 to 0.18% for J_{sc}, V_{oc}, and %η, respectively. Moreover, the theoretical trend of increasing those parameters for DP2-D0 and DP2-D2 is in excellent agreement with the experimental trend.[30]

The η values of the five-membered rings are lower than those of the six-membered rings except DP1-D0, which shows the highest power conversion efficiency of 9.55% due to its larger short-circuit density. However, the addition of three nitrogen atoms in the five-membered ring (DP1-D3) leads to a significant drop in the η values to 3.22%. Overall, using the pyridine (DP2-D1), pyrimidine (DP2-D2), and 1,2,4-triazine (DP2-D3), i.e., the six-membered ring with one, two, and three nitrogen atoms, improves the power conversion efficiency. Also, the cyclopenta-1,3-diene (DP1-D0) shows an excellent performance with an η value up to 9.55%.

4. CONCLUSIONS

In this work, the total power conversion efficiencies for eight DP-based dyes were predicted theoretically, and the estimated parameters included the short-circuit current density (J_{sc}), open-circuit voltage (V_{oc}), and power conversion efficiency (%η). All the estimated data nicely matched the available experimental ones with very small deviations. The results revealed that the η value of the designed dye cyclopenta-1,3-diene (DP1-D0) is predicted to be equal to 9.55%, which is much higher than those of the other designed dyes (DP1-D1, DP1-D2, DP1-D3, DP2-D1, and DP2-D3) and the two experimentally tested ones (DP2-D0 and DP2-D2). The present study suggests new dyes to be carried out by experimentalists as efficient components in fabricated DSSCs. As well, the theoretical chemists' method in designing dyes with improved properties in highly efficient DSSC devices was further validated.

■ ASSOCIATED CONTENT

Supporting Information

The Supporting Information is available free of charge at https://pubs.acs.org/doi/10.1021/acsomega.0c06340.

DFT functional validation; the calculated maximum absorption wavelengths and % deviation; energy diagram for the DSSC including the open-circuit photovoltage and the energy gab; simulated emission spectra of free dyes and UV−vis absorption of adsorbed systems; schematic energy level positions of adsorbed systems, energy gab, and HOMO and LUMO; the *XYZ* coordinates (PDF)

■ AUTHOR INFORMATION

Corresponding Author

Nuha Wazzan − *Chemistry Department, Faculty of Science, King Abdulaziz University, Jeddah 21589, Saudi Arabia;* orcid.org/0000-0002-6313-9400; Email: nwazzan@kau.edu.sa

Author

Ohoud S. Al-Qurashi − *Chemistry Department, Faculty of Science, King Abdulaziz University, Jeddah 21589, Saudi Arabia; Department of Chemistry, Faculty of Science, University of Jeddah, Jeddah 21959, Saudi Arabia*

Complete contact information is available at: https://pubs.acs.org/10.1021/acsomega.0c06340

Notes

The authors declare no competing financial interest.

■ ACKNOWLEDGMENTS

Authors gratefully acknowledge King Abdulaziz University's High-Performance Computing Centre (Aziz Supercomputer) (http://hpc.kau.edu.sa) for assisting in the calculations in this work.

■ REFERENCES

(1) O'regan, B.; Grätzel, M. A low-cost, high-efficiency solar cell based on dye-sensitized colloidal TiO2 films. *Nature* **1991**, *353*, 737−740.

(2) Salimi, H.; Peyghan, A. A.; Noei, M. Adsorption of formic acid and formate anion on ZnO nanocage: a DFT study. *J. Cluster Sci.* **2015**, *26*, 609−621.

(3) Zhang, J.; Li, H.-B.; Sun, S.-L.; Geng, Y.; Wu, Y.; Su, Z.-M. Density functional theory characterization and design of high-performance diarylamine-fluorene dyes with different π spacers for dye-sensitized solar cells. *J. Mater. Chem.* **2012**, *22*, 568−576.

(4) Baviskar, P. K. Low-cost solid-state dye-sensitized solar cell based on ZnO with CuSCN as a hole transport material using simple solution chemistry. *J. Solid State Electrochem.* **2017**, *21*, 2699−2705.

(5) Kay, A.; Grätzel, M. Dye-sensitized core− shell nanocrystals: improved efficiency of mesoporous tin oxide electrodes coated with a thin layer of an insulating oxide. *Chem. Mater.* **2002**, *14*, 2930−2935.

(6) Deogratias, G.; Al-Qurashi, O. S.; Wazzan, N.; Seriani, N.; Pogrebnaya, T.; Pogrebnoi, A. Investigation of optoelectronic properties of triphenylamine-based dyes featuring heterocyclic

anchoring groups for DSSCs' applications: a theoretical study. *Struct. Chem.* **2020**, *31*, 2451−2461.
(7) Al-Qurashi, O. S.; Wazzan, N. A.; Obot, I. B. Exploring the effect of mono- and di-fluorinated triphenylamine-based molecules as electron donors for dye-sensitised solar cells. *Mol. Simul.* **2020**, *46*, 41−53.
(8) Roy, P.; Berger, S.; Schmuki, P. TiO2 Nanotubes: Synthesis and Applications. *Angew. Chem., Int. Ed.* **2011**, *50*, 2904−2939.
(9) Hoyer, P. Formation of a Titanium Dioxide Nanotube Array. *Langmuir* **1996**, *12*, 1411−1413.
(10) Macák, J. M.; Tsuchiya, H.; Ghicov, A.; Schmuki, P. Dye-sensitized anodic TiO2 nanotubes. *Electrochem. Commun.* **2005**, *7*, 1133−1137.
(11) Bandura, A. V.; Evarestov, R. A. From anatase (101) surface to TiO2 nanotubes: Rolling procedure and first principles LCAO calculations. *Surf. Sci.* **2009**, *603*, L117−L120.
(12) Lin, F.; Zhou, G.; Li, Z.; Li, J.; Wu, J.; Duan, W. Molecular and atomic adsorption of hydrogen on TiO2 nanotubes: An ab initio study. *Chem. Phys. Lett.* **2009**, *475*, 82−85.
(13) Gao, X.; Kong, C.-p.; Jia, R.; Jian, W.; Wang, J.; Bai, F.-q.; Zhang, H.-x. Influence of one-dimensional TiO2 nanotube on interfacial electron transfer in dye-sensitized solar cells: Insights from theoretical investigation. *Sol Energy* **2018**, *176*, 545−555.
(14) Ferrari, A. M.; Szieberth, D.; Zicovich-Wilson, C. M.; Demichelis, R. Anatase(001) 3 ML Nanotubes, The First TiO2 Nanotube With Negative Strain Energies: A DFT Prediction. *J. Phys. Chem. Lett.* **2010**, *1*, 2854−2857.
(15) Enriquez, J. I. G.; Moreno, J. L. V.; David, M. Y.; Arboleda, N. B., Jr.; Lin, O. H.; Villagracia, A. R. C. DFT Investigation on the Electronic and Water Adsorption Properties of Pristine and N-Doped TiO2 Nanotubes for Photocatalytic Water Splitting Applications. *J. Electron. Mater.* **2017**, *46*, 3592−3602.
(16) Cui, Y.; Yao, H.; Zhang, J.; Zhang, T.; Wang, Y.; Hong, L.; Xian, K.; Xu, B.; Zhang, S.; Peng, J.; Wei, Z.; Gao, F.; Hou, J. Over 16% efficiency organic photovoltaic cells enabled by a chlorinated acceptor with increased open-circuit voltages. *Nat. Commun.* **2019**, *10*, 2515.
(17) Raga, S. R.; Barea, E. M.; Fabregat-Santiago, F. Analysis of the Origin of Open Circuit Voltage in Dye Solar Cells. *J. Phys. Chem. Lett.* **2012**, *3*, 1629−1634.
(18) Hagfeldt, A.; Boschloo, G.; Sun, L.; Kloo, L.; Pettersson, H. Dye-Sensitized Solar Cells. *Chem. Rev.* **2010**, *110*, 6595−6663.
(19) Zhang, X.; Grätzel, M.; Hua, J. Donor design and modification strategies of metal-free sensitizers for highly-efficient n-type dye-sensitized solar cells. *Front. Optoelectron.* **2016**, *9*, 3−37.
(20) Venkatraman, R.; Panneer, S. V. K.; Varathan, E.; Subramanian, V. Aromaticity−Photovoltaic Property Relationship of Triphenylamine-Based D-π-A Dyes: Leads from DFT Calculations. *J. Phys. Chem. A* **2020**, *124*, 3374−3385.
(21) Lu, T.-F.; Li, W.; Chen, J.; Tang, J.; Bai, F.-Q.; Zhang, H.-X. Promising pyridinium ylide based anchors towards high-efficiency dyes for dye-sensitized solar cells applications: Insights from theoretical investigations. *Electrochim. Acta* **2018**, *283*, 1798−1805.
(22) Wang, X.; Li, Y.; Song, P.; Ma, F.; Yang, Y. Effect of graphene between photoanode and sensitizer on the intramolecular and intermolecular electron transfer process. *Phys. Chem. Chem. Phys.* **2020**, *22*, 6391−6400.
(23) Murakami, T. N.; Koumura, N.; Kimura, M.; Mori, S. Structural Effect of Donor in Organic Dye on Recombination in Dye-Sensitized Solar Cells with Cobalt Complex Electrolyte. *Langmuir* **2014**, *30*, 2274−2279.
(24) Zhao, D.; Saputra, R. M.; Song, P.; Yang, Y.; Li, Y. How graphene strengthened molecular photoelectric performance of solar cells: A photo current-voltage assessment. *Sol Energy* **2021**, *213*, 271−283.
(25) Xu, Y.; Xu, X.; Li, M.; Lu, W. Prediction of photoelectric properties, especially power conversion efficiency of cells, of IQ1 and derivative dyes in high-efficiency dye-sensitized solar cells. *Sol Energy* **2020**, *195*, 82−88.
(26) Lu, T.-F.; Li, W.; Bai, F.-Q.; Jia, R.; Chen, J.; Zhang, H.-X. Anionic ancillary ligands in cyclometalated Ru(ii) complex sensitizers improve photovoltaic efficiency of dye-sensitized solar cells: insights from theoretical investigations. *J. Mater. Chem. A* **2017**, *5*, 15567−15577.
(27) Chaitanya, K.; Ju, X.-H.; Heron, B. M. Can elongation of the π-system in triarylamine derived sensitizers with either benzothiadiazole and/or ortho-fluorophenyl moieties enrich their light harvesting efficiency? − a theoretical study. *RSC Adv.* **2015**, *5*, 3978−3998.
(28) Ma, W.; Jiao, Y.; Meng, S. Predicting energy conversion efficiency of dye solar cells from first principles. *J. Phys. Chem. C* **2014**, *118*, 16447−16457.
(29) Yang, Z.; Liu, C.; Li, K.; Cole, J. M.; Shao, C.; Cao, D. Rational Design of Dithienopicenocarbazole-Based Dyes and a Prediction of Their Energy-Conversion Efficiency Characteristics for Dye-Sensitized Solar Cells. *ACS Appl. Energy Mater.* **2018**, *1*, 1435−1444.
(30) Lin, L.-Y.; Tsai, C.-H.; Wong, K.-T.; Huang, T.-W.; Wu, C.-C.; Chou, S.-H.; Lin, F.; Chen, S.-H.; Tsai, A.-I. Efficient organic DSSC sensitizers bearing an electron-deficient pyrimidine as an effective π-spacer. *J. Mater. Chem.* **2011**, *21*, 5950−5958.
(31) Becke, A. D. Density-functional exchange-energy approximation with correct asymptotic behavior. *Phys. Rev. A* **1988**, *38*, 3098−3100.
(32) Lee, C.; Yang, W.; Parr, R. G. Development of the Colle-Salvetti correlation-energy formula into a functional of the electron density. *Phys. Rev. B* **1988**, *37*, 785−789.
(33) Miertuš, S.; Scrocco, E.; Tomasi, J. Electrostatic interaction of a solute with a continuum. A direct utilizaion of AB initio molecular potentials for the prevision of solvent effects. *Chem. Phys.* **1981**, *55*, 117−129.
(34) Barone, V.; Cossi, M. Quantum calculation of molecular energies and energy gradients in solution by a conductor solvent model. *J. Phys. Chem. A* **1998**, *102*, 1995−2001.
(35) Cammi, R.; Tomasi, J. Remarks on the use of the apparent surface charges (ASC) methods in solvation problems: Iterative versus matrix-inversion procedures and the renormalization of the apparent charges. *J. Comput. Chem.* **1995**, *16*, 1449−1458.
(36) Yanai, T.; Tew, D. P.; Handy, N. C. A new hybrid exchange−correlation functional using the Coulomb-attenuating method (CAM-B3LYP). *Chem. Phys. Lett.* **2004**, *393*, 51−57.
(37) Hay, P. J.; Wadt, W. R. Ab initio effective core potentials for molecular calculations. Potentials for the transition metal atoms Sc to Hg. *J. Chem. Phys.* **1985**, *82*, 270−283.
(38) Frisch, M. J. *Gaussian 09 Programmer's Reference*; Gaussian: 2009.
(39) Dennington, R.; Keith, T.; Millam, J. *GaussView, Version 5*; Semichem Inc.: KS, 2009.
(40) Vlachopoulos, N.; Liska, P.; Augustynski, J.; Graetzel, M. Very efficient visible light energy harvesting and conversion by spectral sensitization of high surface area polycrystalline titanium dioxide films. *J. Am. Chem. Soc.* **1988**, *110*, 1216−1220.
(41) Mandal, S.; Rao, S.; Ramanujam, K. Understanding the photo-electrochemistry of metal-free di and tri substituted thiophene-based organic dyes in dye-sensitized solar cells using DFT/TD-DFT studies. *Ionics* **2017**, *23*, 3545−3554.
(42) Lukeš, V.; Aquino, A.; Lischka, H. Theoretical Study of Vibrational and Optical Spectra of Methylene-Bridged Oligofluorenes. *J. Phys. Chem. A* **2005**, *109*, 10232−10238.
(43) Lin, L.-Y.; Yeh, M.-H.; Lee, C.-P.; Chang, J.; Baheti, A.; Vittal, R.; Thomas, K. R. J.; Ho, K.-C. Insights into the co-sensitizer adsorption kinetics for complementary organic dye-sensitized solar cells. *J. Power Sources* **2014**, *247*, 906−914.
(44) Al-Qurashi, O. S.; Jedidi, A.; Wazzan, N. Single- and co-sensitization of triphenylamine-based and asymmetrical squaraine dyes on the anatase (001) surface for DSSC applications: Periodic DFT calculations. *J. Mol. Graphics Modell.* **2021**, *104*, 107833.
(45) Fu, Y.; Lu, T.; Xu, Y.; Li, M.; Wei, Z.; Liu, H.; Lu, W. Theoretical screening and design of SM315-based porphyrin dyes for

https://doi.org/10.1021/acsomega.0c06340
ACS Omega 2021, 6, 8967−8975

highly efficient dye-sensitized solar cells with near-IR light harvesting. *Dyes Pigm.* **2018**, *155*, 292−299.
(46) Ardo, S.; Meyer, G. J. Photodriven heterogeneous charge transfer with transition-metal compounds anchored to TiO2 semiconductor surfaces. *Chem. Soc. Rev.* **2009**, *38*, 115−164.
(47) Haid, S.; Marszalek, M.; Mishra, A.; Wielopolski, M.; Teuscher, J.; Moser, J.-E.; Humphry-Baker, R.; Zakeeruddin, S. M.; Grätzel, M.; Bäuerle, P. Significant Improvement of Dye-Sensitized Solar Cell Performance by Small Structural Modification in π-Conjugated Donor−Acceptor Dyes. *Adv. Funct. Mater.* **2012**, *22*, 1291−1302.
(48) Cherepy, N. J.; Smestad, G. P.; Grätzel, M.; Zhang, J. Z. Ultrafast electron injection: implications for a photoelectrochemical cell utilizing an anthocyanin dye-sensitized TiO2nanocrystalline electrode. *J. Phys. Chem. B* **1997**, *101*, 9342−9351.
(49) Meade, T. J.; Gray, H. B.; Winkler, J. R. Driving-force effects on the rate of long-range electron transfer in ruthenium-modified cytochrome c. *J. Am. Chem. Soc.* **1989**, *111*, 4353−4356.
(50) Marcus, R. A. On the theory of oxidation-reduction reactions involving electron transfer. I. *J. Chem. Phys.* **1956**, *24*, 966−978.
(51) Davidson, V. L. Electron Transfer Theory. In *Encyclopedia of Biophysics*; Roberts, G. C. K., Ed. Springer Berlin Heidelberg: Berlin, Heidelberg, 2013; pp. 621−625.
(52) Liang, M.; Xu, W.; Cai, F.; Chen, P.; Peng, B.; Chen, J.; Li, Z. New Triphenylamine-Based Organic Dyes for Efficient Dye-Sensitized Solar Cells. *J. Phys. Chem. C* **2007**, *111*, 4465−4472.
(53) Yella, A.; Lee, H.-W.; Tsao, H. N.; Yi, C.; Chandiran, A. K.; Nazeeruddin, M. K.; Diau, E. W.-G.; Yeh, C.-Y.; Zakeeruddin, S. M.; Grätzel, M. Porphyrin-Sensitized Solar Cells with Cobalt (II/III)−Based Redox Electrolyte Exceed 12 Percent Efficiency. *Science* **2011**, *334*, 629.
(54) Marinado, T.; Nonomura, K.; Nissfolk, J.; Karlsson, M. K.; Hagberg, D. P.; Sun, L.; Mori, S.; Hagfeldt, A. How the Nature of Triphenylamine-Polyene Dyes in Dye-Sensitized Solar Cells Affects the Open-Circuit Voltage and Electron Lifetimes. *Langmuir* **2010**, *26*, 2592−2598.
(55) Zhang, J.; Zhu, L.; Wei, Z. Toward Over 15% Power Conversion Efficiency for Organic Solar Cells: Current Status and Perspectives. *Small Methods* **2017**, *1*, 1700258.
(56) Wang, Q.; Ito, S.; Grätzel, M.; Fabregat-Santiago, F.; Mora-Seró, I.; Bisquert, J.; Bessho, T.; Imai, H. Characteristics of high efficiency dye-sensitized solar cells. *J. Phys. Chem. B* **2006**, *110*, 25210−25221.

https://doi.org/10.1021/acsomega.0c06340
ACS Omega 2021, 6, 8967−8975